Red Emissive Carbon Dots as Fluorescent Sensor for Fast Specific Monitoring and Imaging of Polarity in Living Cells

Zheng Yang[a,b,c,*], Hui Li[a,b], Tiantian Xu[b], Mengyao She[a], Jiao Chen[a], Xiaodan Jia[b,c], Ping Liu[a], Xiangrong Liu[b,c], and Jianli Li [a,*]

[a] *Key Laboratory of Synthetic and Natural Functional Molecule of the Ministry of Education, College of Chemistry & Materials Science, Northwest University, Xi'an 710127, PR China*

[b] *College of Chemistry and Chemical Engineering, Xi'an University of Science and Technology, Xi'an 710054, PR China*

[c] *Key Laboratory of Coal Resources Exploration and Comprehensive Utilization, Ministry of Land and Resources, Xi'an 710012, PR China.*

*Corresponding author: yangzheng@xust.edu.cn; orcid.org/0000-0002-1554-4794; lijianli@nwu.edu.cn; orcid.org/0000-0002-4853-7961.

CONTENTS

1. Experimental details.

1.1 Materials:

Citric acid was purchased from Rhawn Chemical Technology (Shanghai, China). L-Methionine and 2,7-dihydroxynaphthalene were purchased from Inno-chem Technology Co. Ethyl acetate was purchased from Zhiyuan Chemical Reagent Co. Sodium chloride was purchased from Damao Chemical Reagent Factory (Tianjin, China). Column chromatography silica gel was purchased from Ocean Chemical Factory (Qingdao, China). All chemical reagents are of analytical grade and can be used directly without treatment.

1.2 Synthesis of CDs:

0.96 g of citric acid, 0.74 g of L-methionine and 0.8 g of 2,7-dihydroxynaphthalene were accurately weighed and poured into a mixture of 20 mL of DMF and 16 mL of deionized water and sonicated for 10 min until completely dissolved. Then put it into a 40ml polyethylene teflon lined autoclave and heated at 160 ℃ for 4 h. After natural cooling to room temperature, the solution was centrifuged at 10,000 r/min for 1 min, and the supernatant was filtered through a 0.2 μm microporous filter membrane to obtain the filtrate. The filtrate was then extracted with a mixture of ethyl acetate and saturated salt water, and washed five times with deionized water at the end. Then the solution was concentrated by spin evaporation and separated by thin layer chromatography using ethyl acetate as the spreading agent (R_f value of 0.59), and the liquid product was dried by spin evaporation to obtain orange-yellow solid powder.

1.3 Characterizations:

The morphology, structure and chemical element characterization of CDs: The transmission electron microscopy (TEM) from JEM-1400 Flash analyzer is used to describe the size and distribution. The power X-ray diffraction (XRD) spectroscopy is employed to investigate the crystallinity (Bruker D8 Advance X-ray diffractometer). The Raman spectroscopy (Thermo Fisher DXR2 spectroscopy) measures the carbon

structure and the degree of disorder, The Fourier transform infrared (FT-IR, Bruker Tensor 27 spectrometer) spectroscopy data are utilized to analyze the different functional groups. The X-ray photoelectron spectroscopy (XPS, PHI-5000VersaProbeIII spectrophotometer) data are evaluated for elemental composition and chemical bonding. The Zeta potential (JS94H microelectrophoresis instrument) is used to judge the charge positivity and negativity. The optical characterization of CDs: The ultraviolet-visible (UV-vis) spectra are performed to analyze chromophores and co-chromophores. The fluorescence intensity can be determined by fluorescence spectroscopy (Horiba FluoroMax 4 fluorescence spectrometer). The decay times (Edinburgh FLS920 steady/transient fluorescence spectrometer) can be calculated to analyze fluorescence lifetime composition. The cytotoxicity test was carried out on ELx800 Absorbance Reader. The cell imaging is collected by Olympus FV1000 confocal microscopy.

1.4 Fluorescence detection of polarity

To inspect the selectivity of CDs to the target, 1.00 mL various ion solutions (10 mmol Ł$^{-1}$) Li^+, Na^+, K^+, Ag^+, Ca^{2+}, Mg^{2+}, Fe^{2+}, Co^{2+}, Ni^{2+}, Cu^{2+}, Zn^{2+}, Mn^{2+}, Cd^{2+}, Hg^{2+}, Pb^{2+}, Fe^{3+}, Cr^{3+}, Al^{3+}, Sn^{4+}, PO_4^{3-}, CO_3^{2-}, OAc^-, $C_2O_4^{2-}$, SO_3^{2-}, Cys, GSH, Hcy, $O_2^{\cdot-}$, H_2O_2, ClO^-, NO, $ONOO^-$, H_2S, adenosine monophosphate (AMP), adenosine diphosphate (ADP), and adenosine triphosphate (ATP) cysteine (Cys), glutathione (GSH), homocysteine (Hcy), ascorbic acid (AA), dopamine (DA), were separately added into 1 mL of CDs solution (1 mg Ł$^{-1}$) and then diluted to 10 mL with distilled water. The obtained solutions were incubated at room temperature for 10 min. The fluorescence emission spectra of the solutions were recorded with a fluorescence spectrometer at an excitation wavelength of 490 nm and slit width of 5 nm.

1.5 Filter paper sensing of polarity

A number of rectangular strips of filter paper were completely immersed in a 1 mg Ł$^{-1}$ CDs solution for one hour and then taken out and allowed to dry completely. Then they were completely immersed in various solvents for one hour and allowed to

stand until completely dried, and these filter papers were placed under a 365 nm ultraviolet (UV) lamp to observe.

1.6 Biological testing

1.6.1. Toxicity testing of the CDs

HepG2 cells were cultured in 96-well plates for 24 h at 37 ℃ and 5% CO_2 (medium was Dulbecco's modified Eagle's medium (DMEM) containing 1% penicillin/streptomycin and 10% fetal bovine serum). The old DMEM was then removed and fresh DMEM with 100 μL of different concentrations of CDs solution (0-100 $\mu g \cdot mL^{-1}$) was added to the cells and incubated for 24 h under same conditions. Then 10 μL of 3-(4,5)-dimethylthiahiazo (-z-y1)-3,5-di-phenytetrazoliumromide (MTT) solution was added to each well and the incubation was continued for 4 h. Finally, the absorbance of each well was recorded using microtiter reader to assess the cytotoxicity of CDs.

1.6.2. Time required for the CDs to enter the cells

As in the above process, the cultured HepG2 cells were added to CDs solution (40 $\mu g \cdot mL^{-1}$) and the pictures were taken at different times (0 s, 20 s, 40 s, 1 min, 2 min, 5 min, 8 min, 12 min, respectively) with confocal laser scanning microscope (CLSM)

1.6.3 Concentration required for the CDs cell imaging

As in the process of culturing cells above, the cultured HepG2 cells were added to different concentrations (0-100 $\mu g \cdot mL^{-1}$) of CDs solution and then they were imaged by CLSM to observe the concentration value corresponding to the cell with the largest fluorescence area.

1.6.4 Subcellular organelle co-localization of the CDs

CDs targeting organelles: As in the process of culturing cells above, the cultured HepG2 cells were incubated with CDs in DMEM for 30 min at 37 ℃, 5% CO_2, and then treated with the commercial dyes LysoTracker (100 nM, targeting lysosomes), NucRed Live 647 (two drops per mL, targeting mitochondria) and Mito-Tracker (100

nM, targeting nuclei) were treated for 30 min. Cells were then washed 3 times with phosphate-buffered (PBS) and 1 mL of serum-free DMEM was added. Cells were finally subjected by confocal laser scanning microscope (CLSM).

1.6.5 Cellular energy-dependent mechanism of the CDs

As the above procedure of culturing cells, the cultured HepG2 cells were incubated with NaN_3 (10 mM) at low temperature for 4 h as the control group, and then the cells cultured with CDs were incubated with the same conditions for another 4 h as the experimental group, and the change of fluorescence intensity of both was observed.

1.6.6. Endocytosis mechanism of the CDs

As in the process of culturing cells above, the cultured HepG2 cells were pretreated with 10 $\mu g \cdot mL^{-1}$ chlorpromazine (CPZ, lattice-protein-mediated endocytosis), 100 $\mu g \cdot mL^{-1}$ goldfinch isoflavin (niche-mediated exocytosis), 10 $\mu g \cdot mL^{-1}$ methyl-β-cyclodextrin (MβCD, lipid raft-mediated endocytosis) and 20 $\mu g \cdot mL^{-1}$ amiloride (microendocytosis) for 4 h, followed by co-culture with 40 $\mu g \cdot mL^{-1}$ CDs solution for 30 min to observe the changes in fluorescence intensity of the 4 groups of cells and to determine the mode of CDs uptake by the cells.

1.6.7 Cell polarity detection by the CDs

As in the process of culturing cells above, the cultured A549, HepG2, and HeLa cells stained with 40 $\mu g \cdot mL^{-1}$ CDs solution were used as the control group. Then A549, HepG2, and HeLa cells stained by 40 $\mu g \cdot mL^{-1}$ CDs solution with the addition of 5 mmol L^{-1} dithiothreitol (DTT) were used as the experimental group, and the change of cell polarity was detected by observing the fluorescence intensity.

2. Optical properties of the probe.

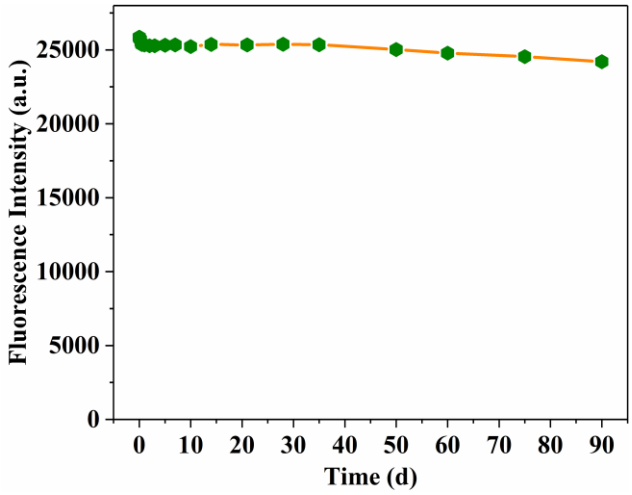

Fig. S1. Fluorescent intensity of CDs at different storage times.

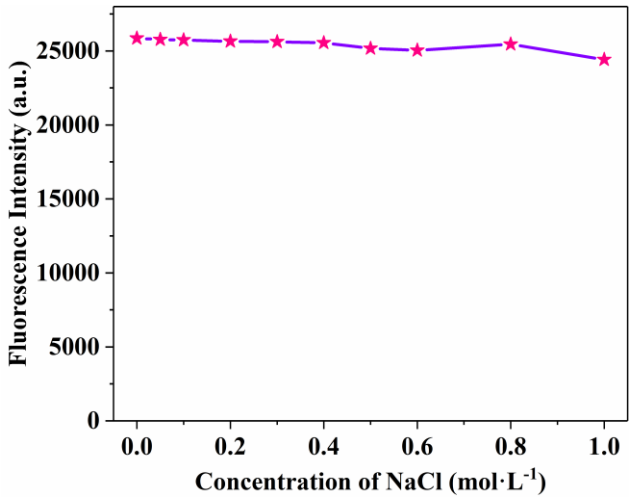

Fig. S2. Fluorescent intensity of CDs at different concentrations of NaCl.

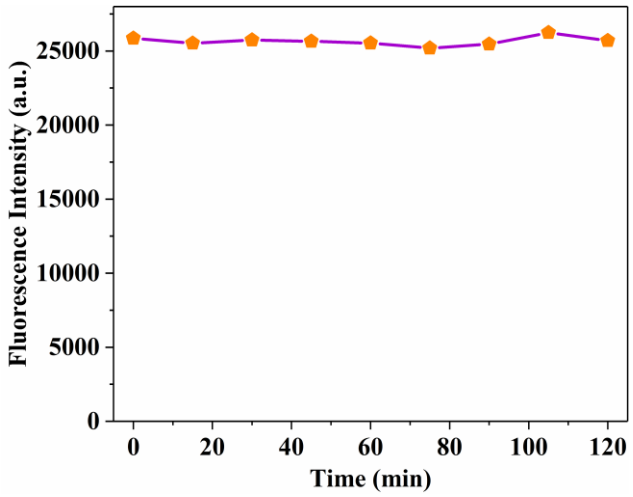

Fig. S3. Fluorescent intensity of CDs at different irradiation time under UV lamp.

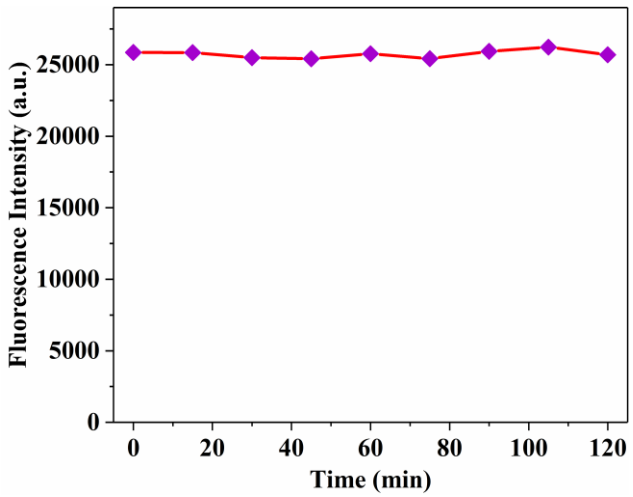

Fig. S4. Fluorescent intensity of CDs at different irradiation time under Xe lamp.

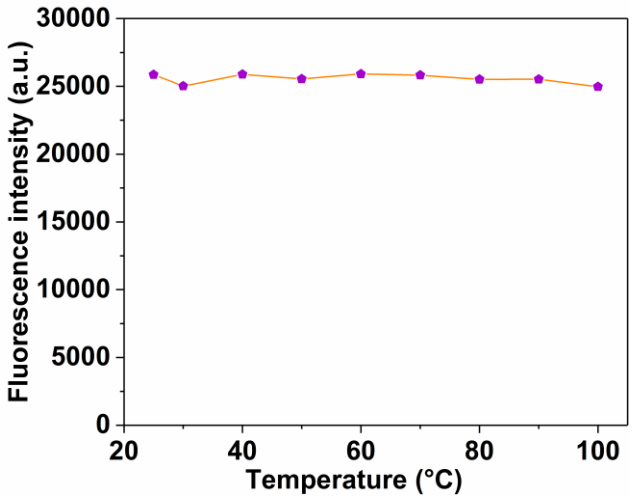

Fig. S5. The fluorescence stability of the CDs in high temperature.

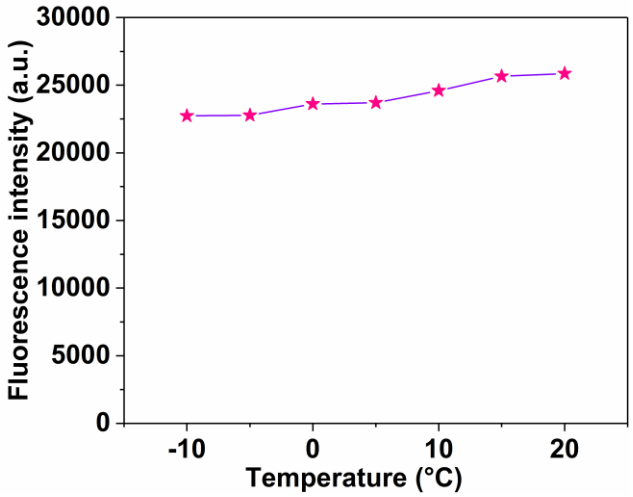

Fig. S6. The fluorescence stability of the CDs in low temperature.

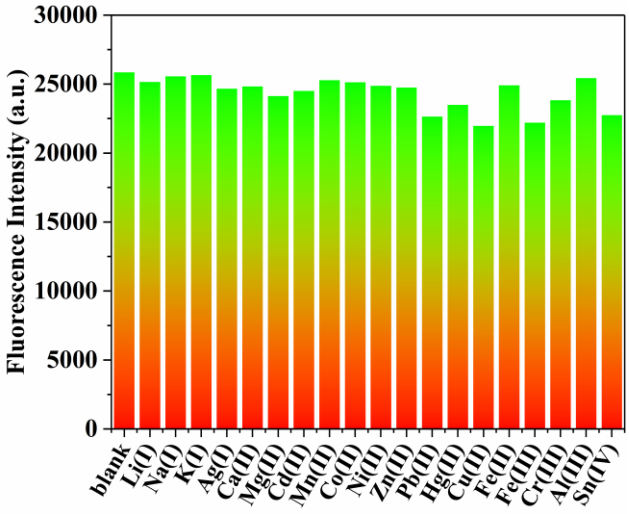

Fig. S7. The fluorescence stability of the CDs in cations.

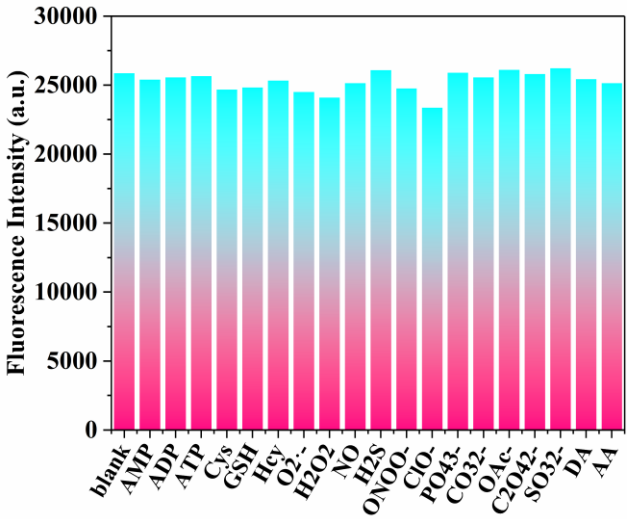

Fig. S8. The fluorescence stability of the CDs in anions and active molecules.

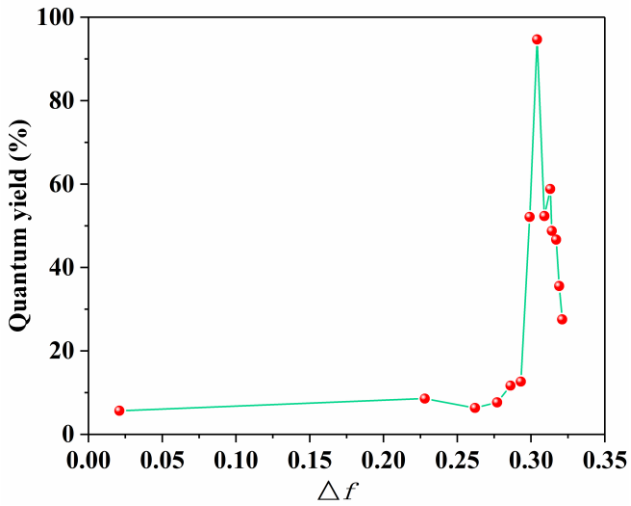

Fig. S9. Fluorescent quantum yields of the CDs in the solvents with different polarity.

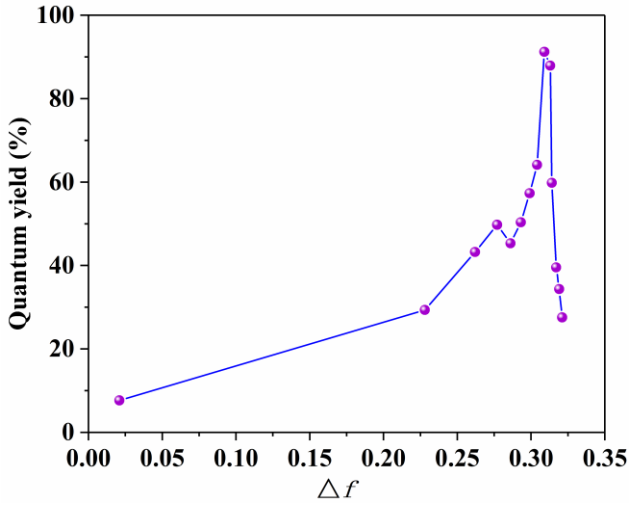

Fig. S10. Fluorescent quantum yields of the CDs and the polarity of different ratios 1,4-dioxane/H_2O mixed solvents.

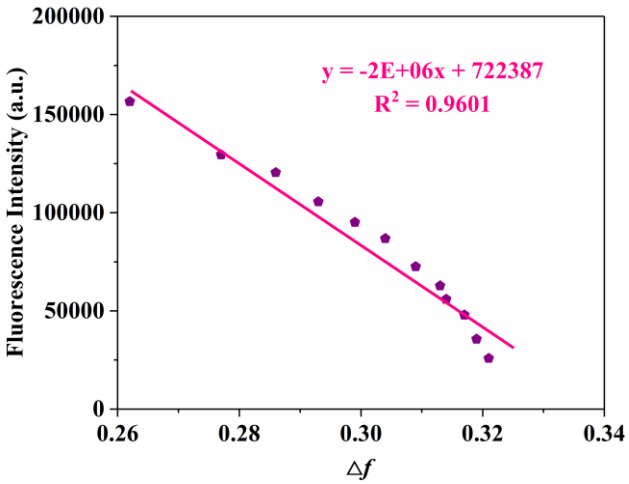

Fig. S11. Linear relationship between fluorescence intensity of the CDs and the polarity of different ratios 1,4-dioxane/H_2O mixed solvents.

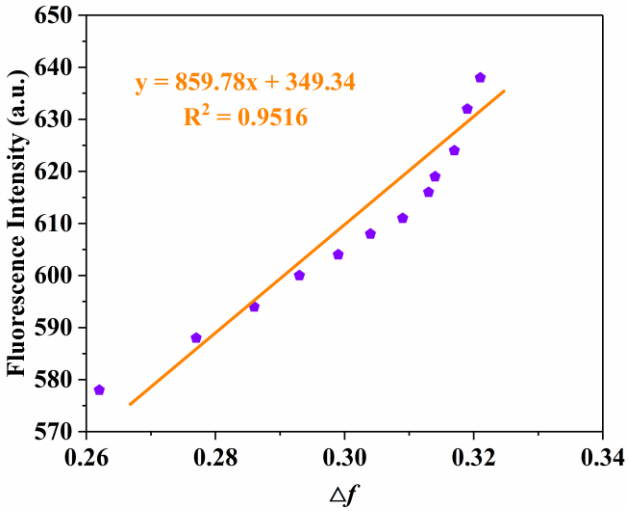

Fig. S12. Linear relationship between fluorescence wavelengths of the CDs and the polarity of different ratios 1,4-dioxane/H_2O mixed solvents.

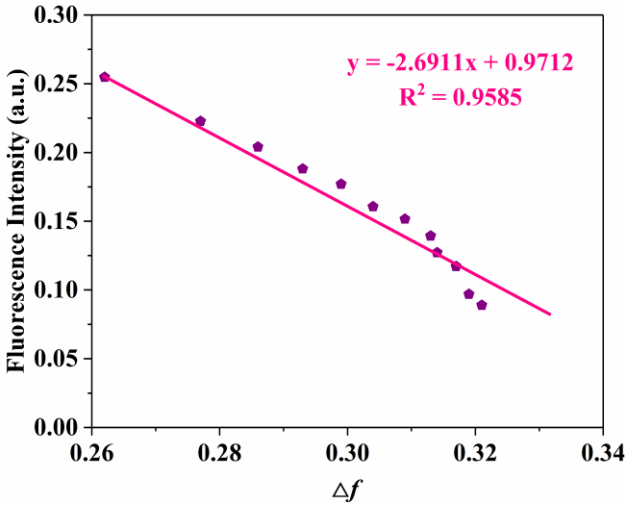

Fig. S13. Linear relationship between absorption intensity of the CDs and the polarity of different ratios 1,4-dioxane/H_2O mixed solvents.

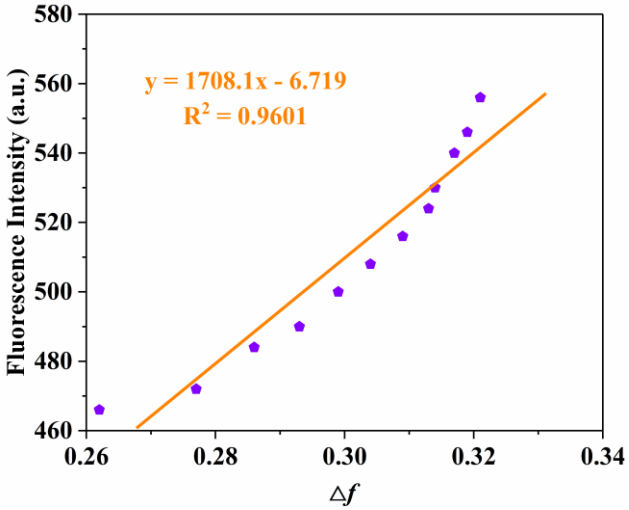

Fig. S14. Linear relationship between absorption wavelengths of the CDs and the polarity of different ratios 1,4-dioxane/H_2O mixed solvents.

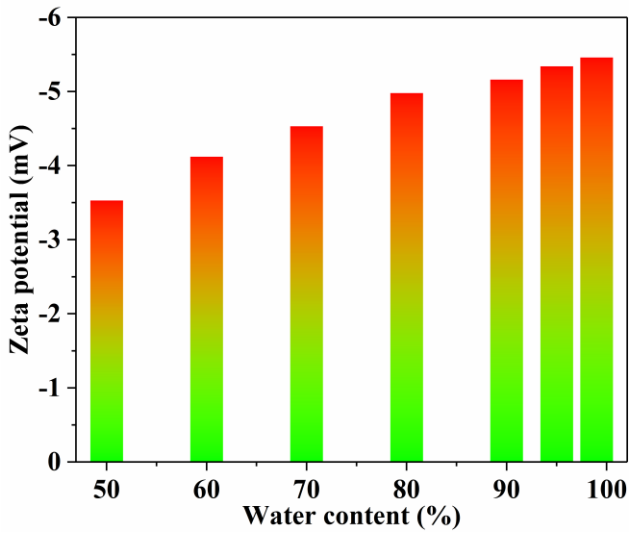

Fig. S15. The Zeta potentials of the CDs in different ratios 1,4-dioxane/H_2O mixed solvents.

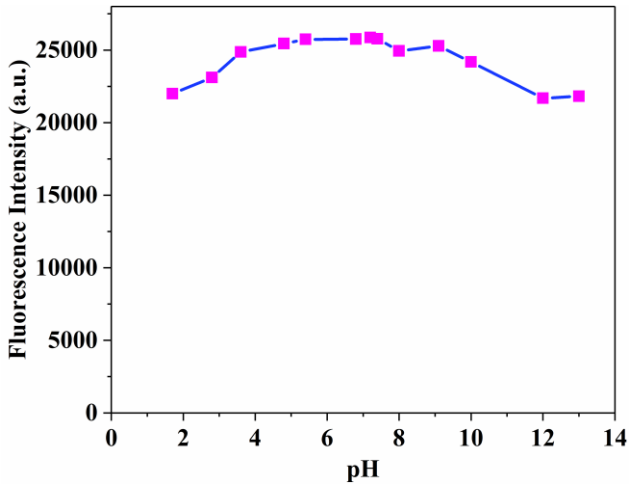

Fig. S16. Fluorescent intensity of the CDs in different pH value.

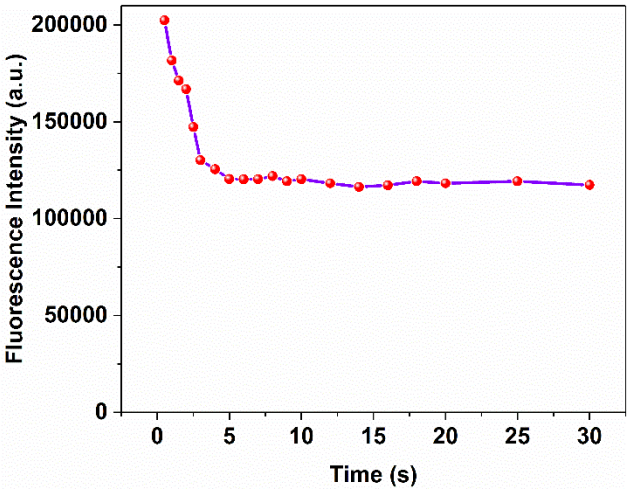

Fig. S17. Response time of fluorescence intensity of CDs to polarity.

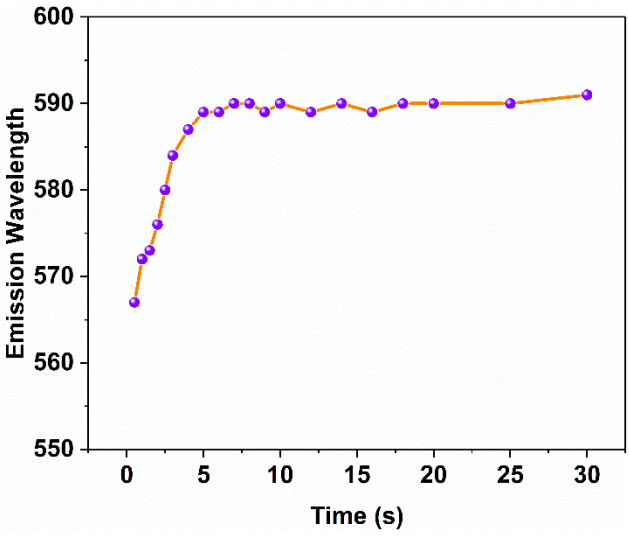

Fig. S18. Response time of emission wavelength of CDs to polarity.

3 Equations about fluorescence lifetime, quantum yield, and polarity.

3.1 Equations for calculation of fluorescence lifetime

$$\tau=\tau_1 B_1 + \tau_2 B_2$$

B_1, B_2 stand for fractional intensities; τ_1, τ_2 are decay times.

3.2 Equations for calculation of quantum yield

$$\varphi_s = \varphi_R \frac{F_S A_R}{F_R A_S} \frac{\eta_S^2}{\eta_R^2}$$

φ stands for the fluorescence quantum yield, F refers to the integrated fluorescence intensity, and A is the absorption values. The subscript "R" and "S" correspond to the reference and the sample.

3.3 Equations for calculation of polarity

For the polarity of different solvents:

$$\Delta f = \frac{\varepsilon - 1}{2\varepsilon + 1} - \frac{n^2 - 1}{2n^2 + 1}$$

ε is represent dielectric constant, n refers refractive index, Δf means polarity.

For the polarity of the different ratios 1,4-dioxane/H_2O mixed solvents:

$$\varepsilon_{mix} = f_a \varepsilon_a + f_b \varepsilon_b$$

$$n_{mix} = f_a n_a^2 + f_b n_b^2$$

$$\Delta f = \frac{\varepsilon_{mix} - 1}{2\varepsilon_{mix} + 1} - \frac{n_{mix}^2 - 1}{2n_{mix}^2 + 1}$$

ε is represent dielectric constant, n refers refractive index, Δf means polarity.

Table S1. Calculated polarity of the solvents and detected absorption and emission wavelengths of the CDs in related solvents.

Sample	Solvent	ε	n^2	Δf [a]	Abs (nm)	Em (nm)
1	Petroleum Ether	1.800	2.008	-0.027	438	531
2	Cyclohexane	2.020	2.034	-0.002	438	532
3	Toluene	2.380	2.238	0.013	438	533
4	1,4-Dioxane	2.219	2.023	0.021	438	541
5	Ethyl Acetate	6.081	1.882	0.201	442	553
6	Tetrahydrofuran	2.510	1.980	0.209	450	560
7	Dichloromethane	8.930	2.029	0.217	458	570
8	Dimethylsulfoxide	47.240	2.184	0.264	470	582
9	Acetone	20.700	1.846	0.284	482	587
10	Dimethyl Formamide	37.780	1.952	0.286	484	594
11	Ethanol	25.320	1.853	0.290	488	598
12	Acetonitrile	36.640	1.804	0.305	508	604
13	Methanol	33.000	1.766	0.309	516	610
14	Water	80.400	1.777	0.321	556	638

a $$\Delta f = \frac{\varepsilon - 1}{2\varepsilon + 1} - \frac{n^2 - 1}{2n^2 + 1}$$

ε is represent dielectric constant, n refers refractive index, Δf means polarity.

Table S2. Calculated polarity of different ratios 1,4-dioxane/H_2O mixed solvents and detected absorption and emission wavelengths of the CDs in related solvents.

Sample	1,4-dioxane	H_2O	ε_{mix} [a]	n^2_{mix} [b]	Δf [c]	Abs (nm)	Em (nm)
1	100%	0%	2.219	2.023	0.021	438	541
2	90%	10%	9.825	1.994	0.228	462	575
3	80%	20%	17.444	1.972	0.262	466	578
4	70%	30%	25.055	1.950	0.277	472	588
5	60%	40%	32.670	1.928	0.286	484	594
6	50%	50%	40.285	1.906	0.293	490	600
7	40%	60%	47.900	1.884	0.299	500	604
8	30%	70%	55.515	1.862	0.304	508	608
9	20%	80%	63.130	1.839	0.309	516	611
10	10%	90%	70.745	1.818	0.313	524	616
11	8%	92%	74.143	1.809	0.314	530	619
12	5%	95%	76.490	1.801	0.317	540	624
13	2%	98%	78.837	1.782	0.319	546	632
14	1%	99%	80.400	1.777	0.320	556	640

a $\varepsilon_{mix} = f_a\varepsilon_a + f_b\varepsilon_b$

b $n_{mix} = f_a n_a^2 + f_b n_b^2$

c $$\Delta f = \frac{\varepsilon_{mix} - 1}{2\varepsilon_{mix} + 1} - \frac{n_{mix}^2 - 1}{2n_{mix}^2 + 1}$$

ε is represent dielectric constant, n refers refractive index, Δf means polarity.

4 Comparison of the CDs with other reported methods

Table S3. Comparison of polarity sensitivity with other reported carbon dots

Carbon dots	LOD	Linear range	Reference
Ps-CDs	0.03	0.03-0.229	[1]
R-CDs	0.013	-	[2]
R-CDs	0.331	-	[3]
R-bCDs	0.02	0.020-0.315	[4]
Phenyl-CDs	0.23	-	[5]
p-CDs	0.189	0.189-0.229	[6]
CDs-3	0.021	0.021-0.320	[7]
N, Cl-CDs	0.093	0.2096-0.3203	[8]
This work	0.021	0.228-0.320	-

Table S4. Comparison of polarity sensitivity with other small molecular sensor

Sensors	LOD	Linear range	Reference
Coumarin	0.186	0.186-0.321	[9]
Mem-C_1C_{18}	0.210	0.210-0.333	[10]
BOB	0..013	0..013-0.32	[11]
N-OH	0.124	0.124-0.316	[12]
CPM	0.209	0.209-0.308	[13]
NIR-BT-P	0.250	0.250-0.298	[14]
CX-P	0.2842	0.2842-0.3167	[15]
DCM-ML	0.229	0.229-0.310	[16]
This work	0.021	0.228-0.320	-

Table S5. Comparison of this CDs with other molecular probes

Method	Properties	Ref
COP	Cell Membrane targeting	[9]
Mem-C_1C_{18}	Cell targeting, enhanced brightness, highly sensitive	[10]
BOB	Mitochondrial targeting, ratiometric imaging	[11]
N-CQDs	High salt tolerance, excellent fluorescence	[17]
N-CQDs	Fast response, acceptable sensitivity	[18]
B/N-CQDS	Water solubility, outstanding photostability	[19]
N-CQDs	Fluorescence quantum yield, abundant surface groups	[20]
CDs	pH sensitivity	[21]
B, N-CQDs	Water solubility, strong fluorescence	[22]
N-CQDs	Low cost	[23]
DPDO-C	Dual-channel emission	[24]
Hcy-Rh	Ratiometric Fluorescent, pH sensitivity, reversible	[25]
DAF	Lipid droplets targeting, excellent quantum yield	[26]
LD-TTP	In vivo, highly sensitive	[27]
Lip-YB	Two-Photon Fluorescent Probe，excellent photostability	[28]
LDs-Red	Red-Emissive, photo-stable	[29]
This work	Polarity sensitivity, fast response, water solubility, outstanding photostability, excellent fluorescence quantum yield, mitochondrial and lysosomal targeting	

5 Calculation details.

The calculations of all the structures were performed with B3LYP function via Gaussian 09 Program. The structures were optimized with a combination of basis of double-ζ quality consisting of 6-31G* for C, H elements, 6-31G** for N, S, O elements. The complex the CDs with Fe^{3+} (S_0 and S_1 state) was optimized with a combination of basis of double-ζ quality consisting of 6-31G* for C, H elements, 6-3G** for N, S, O elements. All the optimized structures were confirmed to be local minimums due to the non-existence of imaginary frequency. Frequency analysis was not performed for excited state on account of the exhausting mumerical calculation of the force constant for such a large system. The environmental effect of the complex was via PCM model with the solvent molecule.

Table S6. The HOMO and LUMO energy and calculated absorption and emission wavelength of the supposed structures of the CDs.

	HOMO (eV)	LUMO (eV)	△ (eV)	Abs (nm)	Opt (nm)
1	-5.17370	-1.65799	-3.51571	305.29	607.58
2	-5.27656	-1.96738	-3.30918	354.09	627.20
3	-5.19792	-2.30889	-2.88903	368.07	641.93
4	-5.93862	-1.99432	-3.94429	335.09	490.72
5	-5.54813	-2.14371	-3.40442	357.17	565.67
6	-5.41806	-1.92630	-3.49177	372.05	582.89
7	-4.97996	-1.73037	-3.24959	325.83	575.32
8	-5.10731	-1.87731	-3.22999	370.95	596.65
9	-5.35003	-2.34317	-3.00686	445.02	867.49
10	-5.11139	-2.29746	-2.81393	436.21	789.07
11	-5.02894	-2.32222	-2.70672	553.53	824.83
12	-5.06295	-2.28712	-2.77583	496.26	770.49

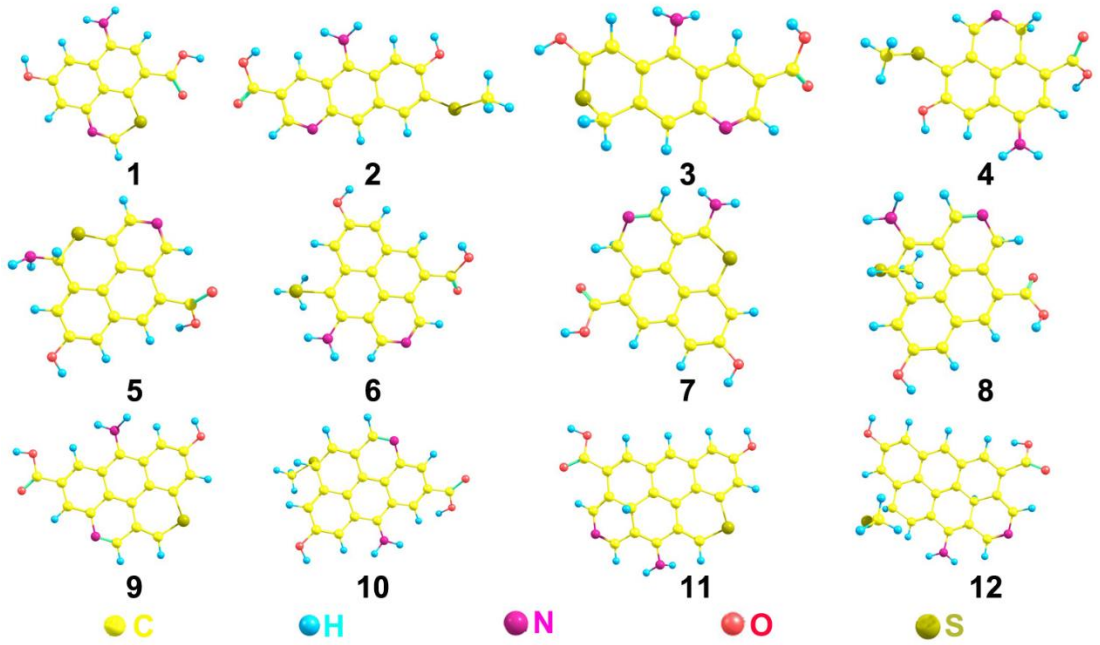

Fig. S19. The optimized structures of the possible structures of the CDs.

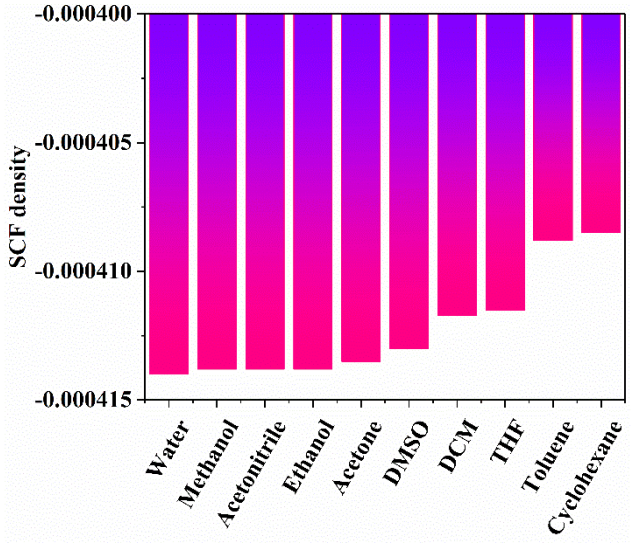

Fig. S20. SCF density of the optimized structure of the CDs in different polarity of solvents.

Table S7. The calculated HOMO and LUMO energy of the CDs at S0 state in solvents with different polarity.

S0	Polarity	HOMO (eV)	LUMO (eV)	△ (eV)
Water	0.321	-5.27656	-1.96738	-3.30918
Methanol	0.309	-5.27847	-1.96766	-3.31081
Acetonitrile	0.305	-5.28010	-1.96793	-3.31217
Ethanol	0.290	-5.28064	-1.96793	-3.31272
Acetone	0.284	-5.28282	-1.96820	-3.31462
Dimethylsulfoxide	0.264	-5.28473	-1.96820	-3.31653
Dichloromethane	0.217	-5.29806	-1.96874	-3.32931
Tetrahydrofuran	0.209	-5.30269	-1.96820	-3.33448
Toluene	0.013	-5.35956	-1.96548	-3.39408
Cyclohexane	-0.002	-5.36799	-1.96738	-3.40061

Table S8. The calculated HOMO and LUMO energy of the CDs at S1 state in solvents with different polarity.

S1	Polarity	HOMO (eV)	LUMO (eV)	△ (eV)
Water	0.321	-4.93071	-2.46671	-2.46399
Methanol	0.309	-4.77016	-2.29229	-2.47787
Acetonitrile	0.305	-4.71859	-2.18222	-2.53637
Ethanol	0.290	-4.72077	-2.16072	-2.56005
Acetone	0.284	-4.74764	-2.15644	-2.59121
Dimethylsulfoxide	0.264	-4.70798	-2.09704	-2.61093
Dichloromethane	0.217	-4.62022	-2.00793	-2.61229
Tetrahydrofuran	0.209	-4.63641	-2.00249	-2.63393
Toluene	0.013	-4.68308	-2.00514	-2.67794
Cyclohexane	-0.002	-4.79057	-2.00188	-2.78869

Table S9. The calculated HOMO and LUMO energy gaps of the CDs in solvents with different polarity.

S1	Polarity	HOMO of S0 (eV)	LUMO of S1 (eV)	△ (eV)
Water	0.321	-5.27656	-2.46671	-2.80985
Methanol	0.309	-5.27847	-2.29229	-2.98618
Acetonitrile	0.305	-5.28010	-2.18222	-3.09788
Ethanol	0.290	-5.28064	-2.16072	-3.11992
Acetone	0.284	-5.28282	-2.15644	-3.12638
Dimethylsulfoxide	0.264	-5.28473	-2.09704	-3.18768
Dichloromethane	0.217	-5.29806	-2.00793	-3.29013
Tetrahydrofuran	0.209	-5.30269	-2.00249	-3.30020
Toluene	0.013	-5.35956	-2.00514	-3.35442
Cyclohexane	-0.002	-5.36799	-2.00188	-3.36612

6 Polarity imaging in living cells.

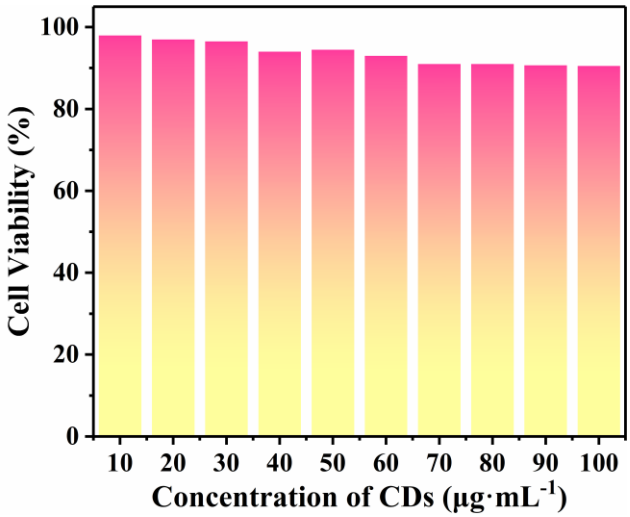

Fig. S21. The influence of cell viability with the change of the CDs concentration

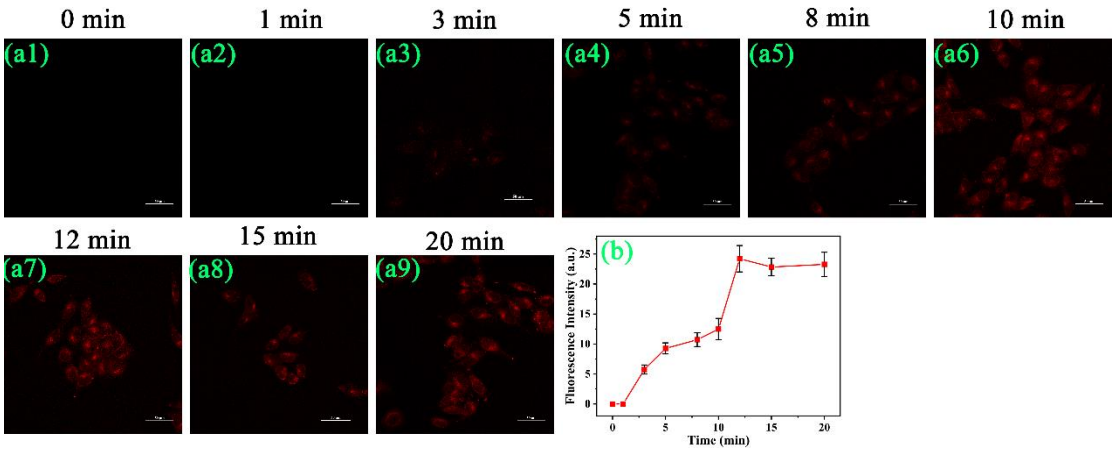

Fig. S22. (a) CLMS images of HepG2 cells treated with 40 μg·mL^{-1} CDs at different times (0−20 min). (b) Corresponding fluorescence intensities of HepG2 cells incubated with CDs for 0−20 min (λex = 514 nm, λem = 540−650 nm) Scale bar: 50 μm.

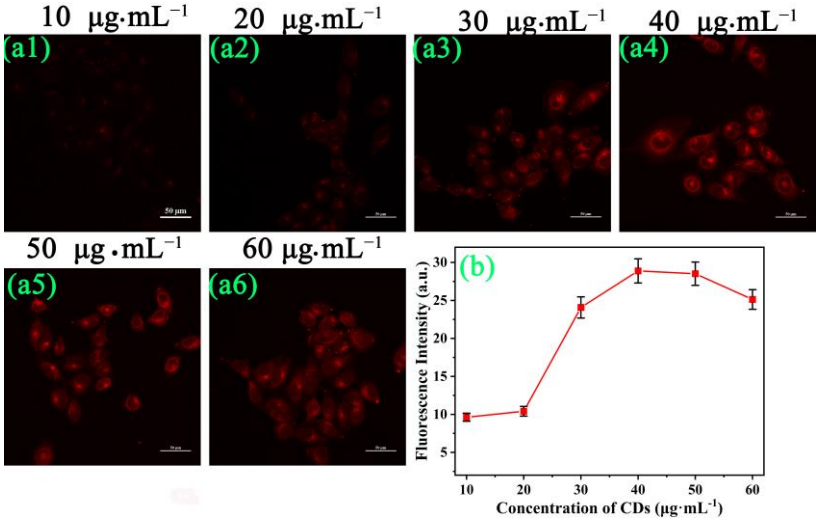

Fig. S23. (a) CLMS images of HepG2 cells treated with different concenrtartion (10−60 μg·mL^{-1}). (b) Corresponding fluorescence intensities of HepG2 cells incubated with CDs for 10−60 μg·mL^{-1} (λex = 514 nm, λem = 540−650 nm) Scale bar: 50 μm.

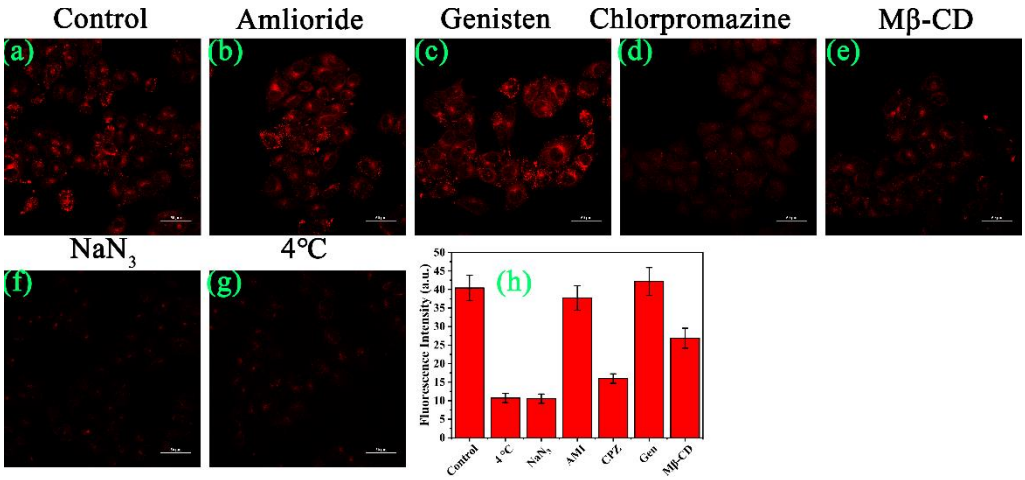

Fig. S24. (a) CLMS images of HepG2 cells incubated with 40 μg·mL^{-1} CDs at 37 ℃. (b-e) CLMS images of HepG2 cells incubated with different endocytosis inhibitors. (f & g) CLMS images of HepG2 cells incubated with 40 μg·mL^{-1} CDs at NaN_3 and 4 ℃. (d) fluorescence intensity of control, CPZ, Mβ-CD, AMI, Gen NaN_3 and 4 ℃ groups. (λex = 514 nm, λem = 540−650 nm). Scale bar: 50 μm.

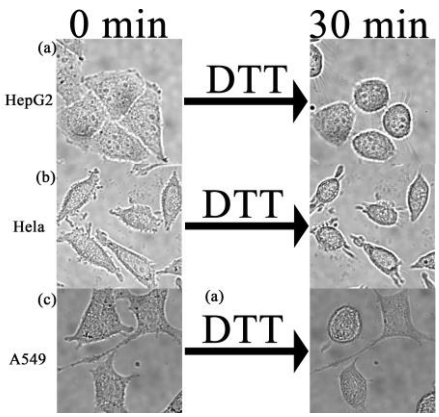

Fig. S25. Bright-field images of HepG2, HeLa, and A549 cells after treatment with 5 mmol L^{-1} DTT for 30 min.

7 References

[1] J. Y. Hu, Y. Q. Sun, X. Geng, J. L. Wang, Y. F. Guo, L. B. Qu, K. Zhang and Z. H Li, *Light Sci. Appl*., 2022, **11**, 185.

[2] X. X. Shi, Y. L. Hu, H. M. Meng, J. Yang, L. B. Qu, X. B. Zhang and Z. H. Li, *Sens. Actuators B Chem.*, 2020, **306**, 127582.

[3] W. Y. Zhou, C. Liu, J. Q. Fan, J. B. Luo, L. H. Liu, J. Q. Huang, R. Y. Liu and X. G. Zhang, *J. Alloys Compd.*, 2022, **920**, 165963.

[4] G. Y. Zou, S. Chen, N. Z. Liu and Y. L. Yu, *Chin. Chem. Lett.*, 2022, **33**, 778-782.

[5] Y. Q. Sun, H. Y. Qin, X. Geng, R. Yang, L. B. Qu, A. N. Kani and Z. H. Li, *ACS Appl. Mater. Interfaces*, 2020, **12**, 31738-31744.

[6] J. H. Liu, Y. Li, J. H. He, D. Yuan, R. S. Li, S. J. Zhen, Y. F. Li and C. Z. Huang, *ACS Appl. Mater. Interfaces*, 2020, **12**, 4815-4820.

[7] E. Shuang, Q. X. Mao, J. H. Wang and X. W. Chen, *Nanoscale*, 2020, **12**, 6852-6860.

[8] J. Jia, W. J. Lu, S. Cui, C. Dong and S. M. Shuang, *Microchim. Acta*, 2021, **188**, 324.

[9] Q. H. Li, J. X. Hong, S. M. Feng, S. Y. Gong and G. Q. Feng, *Anal. Chem.*, 2022, **94**, 11089-11095.

[10] S. Y. Wu, Y. Yan, H. R. Hou, Z. L. Huang, D. X. Li, X. F. Zhang and Y. Xiao, *Anal. Chem.*, 2022, **94**, 11238-11247.

[11] N. Jiang, J. L. Fan, F. Xu, X. J. Peng, H. Y. Mu, J. Y. Wang and X. Q. Xiong, *Angew. Chem. Int. Ed.*, 2015, **54**, 2510-2514.

[12] M. Li, J. L. Fan, H. D. Li, J. J. Du, S. R. Long and X. J. Peng, *Biomaterials*, 2018, **164**, 98-105 .

[13] L. Fan, X. D. Wang, J. Y. Ge, F. Li, X. Wang, J. J. Wang, S. M. Shuang and C. Dong, *Chem. Commun.*, 2019, **55**, 4703-4706.

[14] T. Zhang, F. J. Huo, W. J. Zhang, F. Q. Cheng and C. X. Yin, *Chem. Eng. J.*, 2022, **437**, 135397.

[15] W. X. Wang, Z. Q. Wang, Z. K. Tan, K. Y. Guo, G. J. Mao, Y. Li and C. Y. Li, *Dyes Pigm.*, 2022, **206**, 110612.

[16] X. J. Chao, Y. Hu, R. J. Liu, D. J. Huang and Y. M. Zhang, *Sens. Actuators B Chem.*, 2021, **345**, 130397.

[17] H. W. Ren, M. Y. Li, Y. Z. Liu, T. D. Zhao, R. Y. Zhang and E. D. Duan, *Sci. Total Environ.*, 2022, **811**, 152389.

[18] Z. C. Guo, X. R. Liu, H. Y. Yu, J. F. Hou, S. M. Gao, L. L. Zhong, H. Xu, Y. Yu, J. L. Meng and R. R. Wang, *Spectrochim. Acta A Mol. Biomol. Spectrosc.*, 2021, **257**, 119774.

[19] K. P, A. R. Cherian, U. Sirimahachai, D. A. Thadathil, A. Varghese and G. Hegde, *J. Environ. Chem. Eng.*, 2022, **10**, 107209.

[20] G. Q. Wang, S. R. Zhang, J. Z. Cui, W. S. Gao, X. S. Rong, Y. X. Lu and C. Z. Gao, *Anal. Chim. Acta*, 2022, **1195**, 339478.

[21] Y. M. Zhang, L. Y. Ding, H. W. Zhang, P. Wang and H. J. Li, *Sens. Actuators B Chem.*, 2022, **369**, 132268.

[22] Y. S. Wu, D. M. Qin, Z. Luo, S. Meng, G. C. Mo, X. H. Jiang and B. Y. Deng, *ACS Sustain. Chem. Eng.*, 2022, **10**, 5195-5202.

[23] L. Gu, J. R. Zhang, G. X. Yang, Y. Y. Tang, X. Zhang, X. Y. Huang, W. L. Zhai, E. K. Fodjo and C. Kong, *Food. Chem.*, 2022, **376**, 131898.

[24] S. N. Wang, M. H. Zhou, L. Chen, M. J. Ren, Y. C. Bu, J. J. Wang, Z. P. Yu, X. J. Zhu, J. Zhang, L. K. Wang and H. P. Zhou, *ACS Appl. Bio. Mater.*, 2022, **5**, 3554-3562.

[25] Q. Q. Bai, C. J. Yang, M. J. Yang, Z. Q. Pei, X. B. Zhou, J. X. Liu, H. W. Ji, G. Li, M. M. Wu, Y. L. Qin, Q. Wang and L. Wu, *Anal. Chem.*, 2022, **94**, 2901-2911.

[26] M. Collot, S. Bou, T. K. Fam, L. Richert, Y. Mely, L. Danglot and A. S. Klymchenko, *Anal. Chem.*, 2019, **91**, 1928-1935.

[27] L. Fan, X. D. Wang, Q. Zan, L. F. Fan, F. Li, Y. M. Yang, C. H. Zhang, S. M. Shuang and C. Dong, *Anal. Chem.*, 2021, **93**, 8019-8026.

[28] H. S. Huang, Y. C. Bu, Z. P. Yu, M. T. Rong, R. Li, Z. J. Wang, J. Zhang, X. J. Zhu, L. K. Wang and H. P. Zhou, *Anal. Chem.*, 2022, **94**, 13396-13403.

[29]G. S. Peng, J. N. Dai, R. Zhou, G. N. Liu, X. M. Liu, X. Yan, F. M. Liu, P. Sun, C. G. Wang and G. Lu, *Anal. Chem.*, 2022, **94**, 12095-12102.